

# Practical Encrypted Computing for IoT Clients

McKenzie van der Hagen  
Carnegie Mellon University  
Pittsburgh, U.S.A.  
mckenziv@andrew.cmu.edu

Brandon Lucia  
Carnegie Mellon University  
Pittsburgh, U.S.A.  
blucia@andrew.cmu.edu

**Abstract**—Privacy and energy are primary concerns for sensor devices that offload compute to a potentially untrusted edge server or cloud. Homomorphic Encryption (HE) enables offload processing of encrypted data. HE offload processing retains data privacy, but is limited by the need for frequent communication between the client device and the offload server. Existing client-aided encrypted computing systems are optimized for performance on the offload server, failing to sufficiently address client costs, and precluding HE offload for low-resource (e.g., IoT) devices. We introduce Client-aided HE for Opaque Compute Offloading (CHOCO), a client-optimized system for encrypted offload processing. CHOCO introduces rotational redundancy, an algorithmic optimization to minimize computing and communication costs. We design Client-aided HE for Opaque Compute Offloading Through Accelerated Cryptographic Operations (CHOCO-TACO), a comprehensive architectural accelerator for client-side cryptographic operations that eliminates most of their time and energy costs. Our evaluation shows that CHOCO makes client-aided HE offloading feasible for resource-constrained clients. Compared to existing encrypted computing solutions, CHOCO reduces communication cost by up to 2948 $\times$ . With hardware support, client-side encryption/decryption is faster by 1094 $\times$  and uses 648 $\times$  less energy. In our end-to-end implementation of a large-scale DNN (VGG16), CHOCO uses 37% less energy than local (unencrypted) computation.

## I. INTRODUCTION

Data-producing client devices have a long history of decreasing in size and energy storage capability [1]–[4] leading the way to trillions of tiny devices [5]. As clients scale down, the sophistication of computations on sensor data is scaling up, now often using complex machine learning (ML). With little total energy (potentially no battery) [1]–[4], [6], [7] and constrained compute and memory, a device is fundamentally limited in its local processing capability.

A contrast to local compute is “inference as a service” offloading. A server houses a large collection of DNN models and processes data from many clients, without consuming client memory and energy resources for processing. Such centralized models are easy to evolve, requiring a single update to the model on the server, and avoiding the need to redistribute an updated model to a large network of fielded client devices. *Data privacy* is the main barrier to realizing these benefits of offload computing: offloading exposes sensitive user data to a shared, potentially untrusted offload server.

Recent work offers several options for privacy-preserving computation, including trusted execution environments (TEEs) [8]–[10], differential privacy (DP), multi-party computation (MPC) [11]–[13], and homomorphic encryption (HE) [14]–[17]. Client-aided, hybrid HE-MPC protocols have seen recent success for DNN inference [18]–[21], owing to their ability to use HE to protect user data and process linear operations (e.g. convolution) on encrypted data. Hybrid HE-MPC protocols obfuscate intermediate results of linear operations and send

them to the client, which applies non-linear operations (e.g. activations) using MPC. HE-MPC imposes the high client-side cost of MPC to ensure privacy, not only of client data, but also model data. If an application requires only client data privacy, then HE-MPC needlessly imposes MPC’s cost.

Hybrid HE-MPC implementations of privacy-preserving DNN inference show promising results, but have largely neglected to address the added compute burden on the client. Existing solutions optimize HE-MPC parameters to the benefit of the centralized model server, for both performance and model privacy. Systems choose large ciphertext sizes (MBs), requiring *gigabytes* of client-server communication for a single inference. It is infeasible for resource-constrained client devices, to participate in such schemes.

This work identifies the “middle-ground” between fully-local compute, with its associated resource requirements and inability to use centrally-managed models, and hybrid HE-MPC, with its prohibitive compute and communication costs imposed on client devices for model privacy. We propose Client-aided HE for Opaque Compute Offloading (CHOCO), a system for privacy-preserving computation that minimizes client costs. CHOCO targets applications that do not require model privacy, but that require strict client data privacy. CHOCO reduces client costs by *orders of magnitude* over HE-MPC, availing resource-constrained client devices of the benefits of privacy-preserving ML.

CHOCO is client-aided HE without MPC, performing encrypted linear operations on the server and plaintext non-linear operations on the client. CHOCO introduces *rotational redundancy*, a new encrypted permutation algorithm that minimizes client communication and resource requirements. Additionally, a unique facet of client-aided HE motivates CHOCO: in a typical HE scheme, encryption and decryption happen once per computation, but in client-aided HE, encryption and decryption happen repeatedly on the critical path. We quantitatively show that the prohibitively high time and energy cost to encrypt and decrypt is the client’s primary bottleneck. We propose Client-aided HE for Opaque Compute Offloading Through Accelerated Cryptographic Operations (CHOCO-TACO), a *comprehensive* hardware accelerator implementing all of each of these HE cryptographic primitives and virtually eliminating their time cost.

Our evaluation of a complete hardware-software implementation demonstrates the benefits of a client-optimized system for privacy-preserving computation. Comparing to seven prior HE and/or MPC approaches, CHOCO reduces client communication costs by *orders of magnitude*, with improvements ranging from 14 $\times$ –2948 $\times$ . CHOCO-TACO’s hardware acceleration improves client time and energy by 123.27 $\times$  compared to software and 54.3 $\times$  compared to HEAX, which

accelerates some (but not all) cryptographic sub-operations in hardware. Our results show that CHOCO makes client-privacy-preserving DNN inference comparably performant to local inference (using TFLite), sometimes even *exceeding* the performance of local inference, while avoiding the limitations of fully-local compute. Our main contributions are:

- CHOCO, a client-optimized system for privacy-preserving computation enabling encrypted computing for resource-constrained devices.
- Rotational redundancy, an encrypted permutation algorithm that minimizes client-server communication.
- CHOCO-TACO, a specialized hardware accelerator for client-side HE primitives.
- A full hardware-software implementation of client-aided privacy-preserving DNN inference that improves client costs by orders of magnitude compared to HE-MPC, performing comparably to local computation, while enjoying the benefits of model centralization.

## II. BACKGROUND & MOTIVATION

CHOCO allows an IoT device to offload computation to a more-capable server that computes on encrypted data using Homomorphic Encryption (HE). Primitive operations, most of which support encrypted, Single Instruction Multiple Data (SIMD) computation, are composed into HE algorithms. These algorithms are in turn used to build encrypted HE applications, such as DNN inference.

### A. Homomorphic Encryption

Homomorphic encryption is a class of cryptography schemes that allow computing on encrypted data. In HE, for a pair of messages  $m_1$  and  $m_2$  that can be manipulated by an operation  $\oplus$ , a homomorphic version of the operation  $\oplus'$ , and encryption/decryption operations,  $Enc()$ ,  $Dec()$ , the homomorphic operation applied to the encrypted data produces a result that, when decrypted is equal to the operation applied to unencrypted data:

$$Dec(Enc(m_1) \oplus' Enc(m_2)) = m_1 \oplus m_2 \quad (1)$$

Modern HE schemes [22], [23] are based on the ring learning with errors problem (RLWE). These schemes encrypt a *vector* of thousands of values into the coefficients of a large polynomial, hiding the vector’s contents through modular arithmetic and the addition of noise. The HE operations in Table I manipulate ciphertexts, producing new ciphertexts containing the result of an operation applied element-wise to the input as depicted in Figure 1. Each operation adds a predictable amount of noise to the encrypted vector, with some operations (e.g., multiplication) adding a large amount of noise, and others (e.g., addition) adding little. The arithmetic depth of an HE computation is limited by noise growth. A sequence of operations that exhausts the noise budget renders decryption impossible and data unrecoverable. To avoid exceeding the noise budget, a system must schedule encrypted operations to limit noise growth.

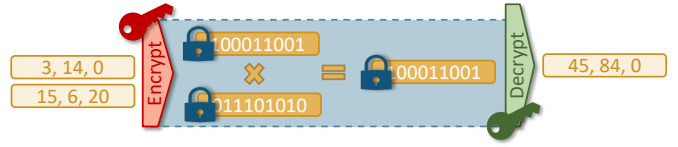


Fig. 1: Homomorphic Encryption allows for computation directly on encrypted vectors of data.

TABLE I: Homomorphic Encryption Operations: The operations available in homomorphic encryption along with their computational complexity and relative noise growth. All operations are performed with a ciphertext, i.e. a plaintext multiply denotes the multiplication of a plaintext with a ciphertext.

Operation	Complexity	Noise Growth
Encrypt	$O(N \times \log N \times r)$	N/A
Decrypt	$O(N \times \log N \times r)$	N/A
Plaintext Add	$O(N \times r)$	Small
Ciphertext Add	$O(N \times r)$	Small
Plaintext Multiply	$O(N \times \log N \times r)$	Moderate
Ciphertext Multiply	$O(N \times \log N \times r^2)$	Large
Ciphertext Rotate	$O(N \times \log N \times r^2)$	Small

HE can *refresh* a ciphertext to eliminate accumulated noise, replenishing the full budget. *Fully* Homomorphic Encryption (FHE) refreshes noise without decryption at enormous computational cost through “bootstrapping” [24]. In contrast, *Somewhat* Homomorphic Encryption (SHE) [18], [23], [25]–[27] refreshes noise with pre-scheduled decryption and re-encryption operations.

TABLE II: Homomorphic Encryption Parameters for the BFV Scheme [25], [26], [28]

Parameter	Name	Description
$N$	Poly. Mod.	# of coeffs per ciphertext.
$q$	Coeff. Mod.	Max value of ciphertext coeff.
$k$	# Coprime Mod.	Number of moduli in RNS
$\{k\}$	Coprime Mod. Bits	Bits per coprime mod.
$w$	Word Size	Bytes per encrypted coeff.
$t$	Plaintext Mod.	Max value of plaintext coeff.
$s$	Ciphertext Components	# polynomials per ciphertext

CHOCO uses the increasingly practical Brakerski/Fan-Vercauteren (BFV) SHE scheme [25], [26] in SEAL [27]. Table II summarizes the scheme’s parameters, which dictate its security, computational complexity, noise budget, and ciphertext size:

$$w \times N \times s \times (k - 1) \quad (2)$$

Typically, the polynomial modulus,  $N$ , is a power of two between  $2^{11}$  and  $2^{15}$ . A fresh ciphertext is two polynomials ( $s = 2$ ) of  $N$  elements each. For a given  $N$ , a smaller coefficient modulus  $q$  provides higher security but a smaller noise budget. A practical  $q$  value is hundreds of bits. Operating directly on such large values is inefficient; HE schemes use the Residual Number System (RNS) [29] to represent numbers

using  $k$  smaller, co-prime moduli. SEAL uses 60-bit residual moduli, to fit in a 64-bit machine word.

BFV supports integer operations modulo the plaintext modulus  $t$ . A larger  $t$  allows for larger numbers but contributes to a smaller noise budget. Parameter selection is application-dependent and must allow for sufficiently large plaintext values while maintaining a budget for sufficient noise growth. Table III shows CHOCO’s parameters and ciphertext size, in bytes.

TABLE III: HE Parameter Selections: All parameters are chosen to satisfy at least 128-bit security.

Label	$N$	$\log_2 q$	$\{k\}$	$\log_2 t$	Size (B)
A	8192	175	{58,58,59}	23	262,144
B	4096	109	{36,36,37}	18	131,072

### B. Homomorphic Algorithms

Primitive HE operations presented in Table I allow for SIMD arithmetic to be performed on large vectors. These fundamental operations compose to support computations such as convolution or matrix multiplication. Algorithms using HE primitives come in two varieties depending on how inputs are encoded into ciphertexts. *Batching* algorithms, optimized for throughput, encode a single data point from thousands of inputs into a single ciphertext vector and exploit natural SIMD operations [16], [30]. Alternately, *packed* algorithms, optimized for latency, encode multiple data points from a single input as a ciphertext vector and utilize permutations to properly align and operate on the desired points [14], [18].

### C. Homomorphic Applications

HE theoretically supports arbitrary functions (through mapping to polynomials at extremely high computational cost [15]), however, practical HE applications use HE primitives directly and are arithmetic-depth-limited. Prior work has identified ML inference using deep neural networks (DNNs) as a compelling use of HE, because of its structured form and complete reliance on simple linear algebra.

Early work on HE for ML performed all computation on encrypted data [14], [16], [30], communicating with the source of the data only to receive initial inputs and return final results. Unfortunately, these techniques have limited applicability to large and complex networks because of their modified activation functions, large noise growth across multiple layers, and subsequent reliance on very large parameter selections [15]. This directly results in ciphertext sizes of multiple megabytes, inflating both computation and communication costs to impractical levels.

As an alternative, recent solutions have focused on *client-aided* HE [17], [18], [21]. In these protocols, the natural linear algebra capabilities of HE are used to perform convolution and fully-connected layers on the offload server. The client is then enlisted to perform all non-linear activation and pooling operations. Intermediate results are communicated at layer boundaries and computation continues back-and-forth until the entire network is completed.

Client-aided HE has been shown to boast multiple benefits. By avoid modified activation functions, they allow for privacy-preserving inference on pre-trained networks. Furthermore, by sending data back to the client for some operations, client-aided HE regularly refreshes the ciphertext noise budget. Thus, client-aided HE does *not* limit DNN depth, and does *not* require extremely costly HE parameter settings. These benefits, however, come at the cost of increased client responsibility, especially for the abundant decryption and re-encryption operations. The client-side costs are the central impediment to the adoption of client-aided HE for IoT devices. CHOCO aims to break this participation barrier through encrypted algorithm optimization and architectural acceleration.

### D. Motivation for Client-Aware Optimization

Client-aided privacy-preserving computation places an enormous burden on resource-constrained IoT client devices. The computational costs intrinsic to the client-aided model motivate our work on client-optimized software and hardware support.

Interaction with the client is used to refresh the ciphertext noise budget and compute (relatively inexpensive) non-linear activation and pooling operations in plaintext. To do so, the system regularly exchanges data with the client to be decrypted, minimally computed on, and re-encrypted. This process has an important net effect on client responsibility: *abundant encryption and decryption operations are on the critical path*. These cryptographic operations in software are extremely computationally costly, even using a highly-optimized commercially available implementation [27].

We used our end-to-end software-only client-aided prototype to measure the cost of encryption and decryption in real encrypted neural network implementations. The software baseline system (which we describe in detail in Section III) utilizes existing server-optimized encrypted algorithms from [18] and default parameter selections from [27]. We measure the time to complete a single classification inference using each of four full-fledged DNN models (we describe our methodology in detail in VI-A).

Figure 2 shows the time spent computing on the client, running encrypted computation on the offload, and communicating. As model size increases, communication and client computation cost increases. Encrypted computation cost at the offload device is consistently very time consuming. A rich and complementary line of work in server-optimized encrypted algorithms [14], [17]–[21] and hardware support [31]–[33] is expected to continue reducing these costs, but the goal of our work is *not* to optimize offload-side HE. Instead, we focus on reducing the costs in time (and commensurately in energy) on the client side. Minimally addressed by prior work [34], we approach this pursuit with specific attention toward realistic applications (e.g. parameters selections) and IoT devices (e.g. low-power).

The compute costs on the client side are primarily the work of encryption and decryption. Figure 3 shows a breakdown of time spent by the client during these DNN inference

computations. Over 99% of the client’s time is HE operations, rather than ML operations (i.e., non-linear computation & quantization). The plot also shows that existing hardware support for the Number Theoretic Transform (NTT) and Dyadic Multiplication, such as that provided in HEAX [31], is not sufficient to reduce the cost of encryption. We profiled the encryption and decryption computations in SEAL to determine that these operations only account for about 50% of the total runtime. We optimistically modeled the benefit of hardware support for both sub-operations by scaling our software runtime accordingly by the speedup factor reported in the original HEAX paper. Even with the modular benefits of HEAX and other offload-side accelerators [31]–[33], encryption and decryption time spent by the client remains dominant by orders of magnitude over ML computations. Often dismissed as insignificant one-time costs, encryption and decryption are on the critical path in the client-aided model and demand further optimization via client-optimized encrypted algorithms and comprehensive hardware support. In this work, we develop such support, making client-aided encrypted inference feasible and favorable for resource-constrained IoT clients.

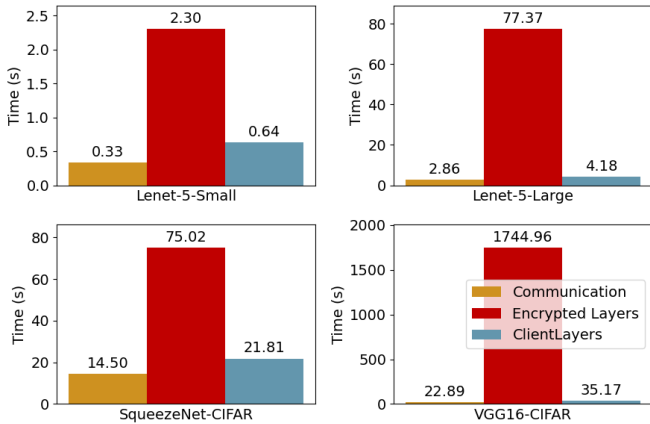


Fig. 2: Complete runtime in seconds for single image inference on each network.

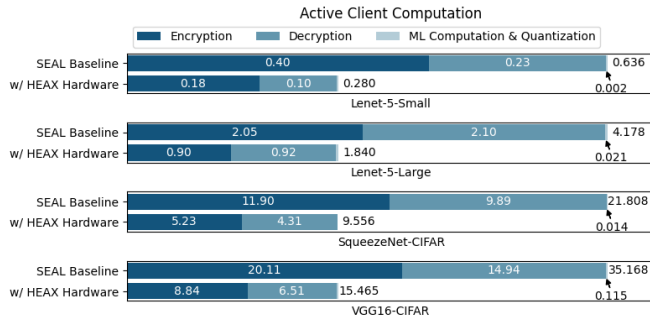


Fig. 3: Breakdown of client execution time in seconds using SEAL software with the default parameter settings on an unmodified ARM core and with hardware support for limited operations from [31]

### III. CLIENT-OPTIMIZED CLIENT-AIDED HE

CHOCO is a client-optimized system model and implementation for client-aided encrypted computation. The model assumes a resource-constrained client device and a more computationally capable, but untrusted, shared offload server. Typical of HE systems, we assume a semi-honest adversary model for the offload device: the adversary may be curious about the input data, but the system is trusted to faithfully perform the specified operations. In contrast to computationally expensive MPC protocols, CHOCO does not make any attempt to hide data on the offload device from the client, including pre-trained ML model data. Rather, the priority of CHOCO is to provide strong privacy guarantees for sensitive client data from IoT devices.

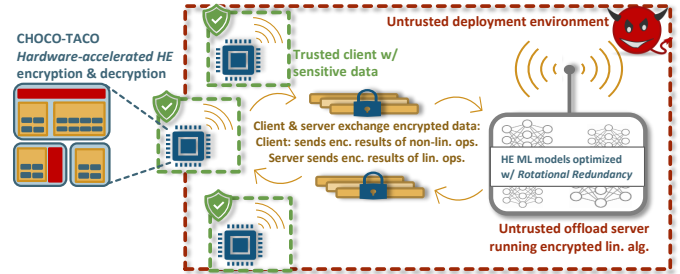


Fig. 4: System architecture for CHOCO. A resource-constrained sensor device and an untrusted offload device communicate via ciphertexts to collaboratively and securely process sensitive data.

CHOCO implements client-aided HE offloading, partitioning work layer-by-layer between the client and the offload device. It optimizes cryptographic algorithms developed in prior work and tunes cryptographic parameters to make feasible the amount of client work performed. CHOCO introduces *rotational redundancy*, which is a new approach to permuting a vector of data encrypted in a ciphertext, which is useful for matrix manipulations such as convolution. The technique reduces the noise growth imposed by common rotation operations, allowing for smaller parameter selections and correspondingly smaller ciphertexts.

#### A. Selecting Efficient HE Parameters

Choosing appropriate HE parameters (as introduced in Section II-A) is a vital yet cumbersome step of encrypted application development [15]. The selection of different parameters leads to different ciphertext size and noise characteristics, which, in turn, influence computation, encryption, decryption, and communication costs in the client-aided model. A system can achieve the same security level with different parameters (e.g. different ciphertext sizes). As such, CHOCO actively minimizes parameter selection via quantization and encrypted algorithm optimization.

An HE scheme’s plaintext modulus  $t$  defines the number of bits in which to store each plaintext value within each element of an encrypted vector. CHOCO quantizes data into fewer bits before encrypting, because when tolerable, quantization to fewer bits allows the use of a smaller plaintext modulus.

As shown by the varying  $t$  values in Table IV, this increases a ciphertext’s noise budget without changing its size, incentivizing the smallest possible  $t$  that does not overflow [35]. Our CHOCO prototype quantizes signed floating point input values to a 4-bit range. The sequentially applied HE operations of convolution then expand these values up to (but not over) our 23-bit prime coefficient modulus value. When a ciphertext is refreshed at layer boundaries the data is also requantized to 4-bits.

### B. HE Algorithm Optimization

CHOCO uses the cryptographic primitives from the SEAL encrypted computing library [27] to implement the HE algorithms developed in Gazelle [18]. These HE algorithms correspond to encrypted linear algebra operations used, for instance, in DNN inference. In CHOCO, all of these encrypted computations execute on the offload device.

Introduced in Section II-B, Gazelle implements *packed* homomorphic algorithms which require permutations for rearranging input elements within an encrypted vector. In this way, elements are appropriately aligned for matrix manipulations such as 1-D, 2-D, and strided convolutions [18]. A key challenge presented by arbitrary permutations is that each requires a sequence of encrypted vector rotation and masking multiplication operations [36]. The depth of such operations quickly deplete the limited noise budget of a ciphertext.

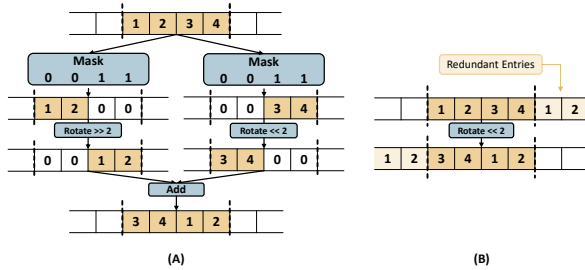


Fig. 5: Encrypted windowed rotation using arbitrary permutation (A) and rotational redundancy (B)

Rotational redundancy is a new way to perform certain permutations on an encrypted vector. The technique targets *windowed rotation* permutations that rotate the elements in a sub-range of a vector, wrapping elements around from the top of the sub-range to the bottom and vice versa. This is in contrast to naturally supported HE rotations which can only rotate the vector in its entirety. Figure 5 shows a windowed rotation permutation on a ciphertext. The standard implementation (A) uses both rotations and masking multiplications, quickly exhausting the ciphertext’s noise. In contrast, implementation (B), introduced in CHOCO, uses rotational redundancy to perform such a permutation with only a single relatively low-cost encrypted rotation. The key to rotational redundancy is to pack the window of values to be rotated with additional redundancy on either side *before* encryption. The redundancy contains the in-window elements that would “wrap around” when the permutation executes. After a series of windowed

rotations and other operations, values outside the window of interest are simply ignored upon decryption. The amount of redundancy required for a windowed rotation corresponds to the amount of rotation to be performed, and, for the rotations used in convolutions, is typically a small fraction of the vector size. Rotational redundancy trades the use of more space in a vector for slower depletion of ciphertext noise, and in turn enables the use of smaller parameter selections. Table IV quantifies these benefits.

TABLE IV: Noise Budget: The initial noise budget of a ciphertext varies with different selections of  $N$ ,  $\log_2 t$ , and  $\{k\}$ . The noise budget remaining after a single rotation versus an arbitrary permutation with masking also demonstrates the benefit of rotational redundancy in eliminating masking multiplies.

Parameters	Initial	After Rotate	After Permute
8192, 20, {58,58,59}	68	66	42
8192, 23, {58,58,59}	62	59	33
8192, 28, {58,58,59}	52	50	18
4096, 16, {36,36,37}	33	31	12
4096, 18, {36,36,37}	29	26	5
4096, 20, {36,36,37}	25	22	0

In our neural network image classification implementation, a ciphertext vector is the concatenation of a vector per channel in the image. Executing inference requires windowed rotation within each channel. We pack images, adding rotational redundancy to each channel. By then packing channels into evenly spaced power-of-two slots in the ciphertext, the alignment of entire channels can also be achieved with simple encrypted rotations and no masking multiplies. Ultimately, convolution is achieved with optimal multiplication efficiency - a single multiplication of the weights with the inputs.

After all algorithm and parameter optimizations, CHOCO utilizes freshly encrypted ciphertexts with only 2 prime residues, a 50% reduction in ciphertext size from the SEAL default parameters for  $N = 8192$ . Half of that improvement, the elimination of one entire residue, is from rotational redundancy alone. As discussed in Section VI, this reduction in ciphertext size has a direct and dramatic benefit in both computation and communication costs.

## IV. HARDWARE ACCELERATION

CHOCO-TACO is a hardware accelerator for homomorphic encryption and decryption operations, designed for client-aided HE. Figure 3, shows that accelerating NTT/INTT and dyadic multiplication [31] only is insufficient in reducing the dominating costs of these cryptographic primitives. CHOCO-TACO, by contrast, effectively accelerates all of the component functions that make up HE encryption and decryption, which we demonstrate through a worked example in Section IV-C and show quantitatively in Section V.

### A. BFV Encryption

$$Enc([P0, P1], m) = ([\Delta m + P0u + e1]_q, [P1u + e2]_q) \quad (3)$$

where  $u \xleftarrow{\$} R_2$  and  $e1, e2 \leftarrow \chi$

CHOCO-TACO accelerates asymmetric BFV encryption, described by Equation 3 [28], where  $m$  is a message to encrypt,  $P_0, P_1$  are public keys, and  $u, e_1, e_2$  are vectors of randomly sampled numbers. Figure 6 fully diagrams the RNS implementation of equation 3 from SEAL [27]. The algorithm encrypts a message by first producing an encrypted "zero" by combining the vectors of randomly sampled numbers with the public keys through coefficient-wise multiplication and addition. The encoded message is then added to the encrypted zero to produce the final ciphertext.

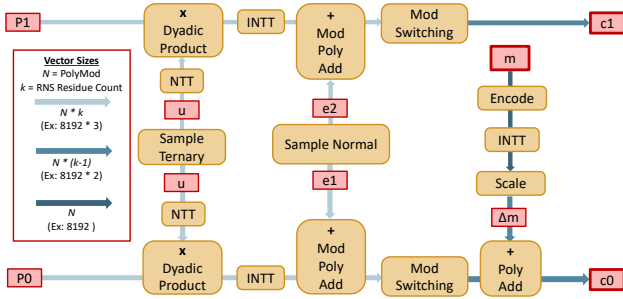


Fig. 6: Pipeline of the BFV encryption operation to sample random noise, scale the input message, and ultimately create a ciphertext of two polynomials, each in RNS form. [28], [32]

## B. Encryption Architecture

CHOCO-TACO accelerates each of the main sub-operations that make up BFV encryption and decryption. CHOCO-TACO is a parallel, pipelined accelerator that directly implements the BFV algorithm. Figure 7 shows the full encryption and decryption accelerator. The design has several key *modules*: Random Number Generation, Polynomial Multiplication, Polynomial Addition and Modulus Switching, and Message Encoding. Each module contains functional blocks, which may be replicated for parallelism, and memory necessary to perform each operation. Each functional block contains an array of processing elements to allow for data parallelism within a functional block. The design additionally pipelines operations within and across modules.

1) *Random Number Generation*: CHOCO-TACO has a dedicated RNG module that implements the Blake3 [37] cryptographic hashing algorithm. The CHOCO-TACO configuration in Figure 7, requires this module to produce 565 MB/s of random values at peak and 201 MB/s on average. The RNG module is also responsible for interpreting the provided randomness as an integer from either a ternary or normal distribution, which it transforms into RNS form. We upgraded our software encryption implementation to use Blake3 instead of Blake2, giving the algorithmic performance increases to both CHOCO-TACO and the baseline.

2) *Polynomial Multiplication*: CHOCO-TACO includes a module for polynomial multiplication of two polynomials, like prior work [31]–[34]. The module transforms the polynomials to NTT form, then performs element-wise dyadic product. The module converts the result back to a polynomial using INTT. CHOCO-TACO’s NTT and INTT modules are conceptually

similar to HEAX [31]. The modules perform pipelined SIMD memory accesses, following the NTT’s butterfly dataflow pattern.

The hardware computes polynomial multiplication of the RNS form of  $u$  and each public key,  $P_0$  and  $P_1$ . SEAL stores public keys in NTT form, so only the single NTT transformation for  $u$  is supported in hardware. NTT’s butterfly dataflow requires access to an entire polynomial at once, precluding aggressive pipelining (i.e., forwarding partial results). Once  $u$  is entirely transformed, results flow to the dyadic product block along with  $P_0$ , and  $P_1$ . Both ciphertext components ( $c_0$  and  $c_1$ ) use the same NTT encoding of  $u$ , allowing it to remain in the NTT working buffer throughout encryption. Dyadic multiply results flow to a separate INTT buffer. After all outputs accumulate, the hardware performs in-place INTT, producing a result.

3) *Polynomial Addition and Modulus Switching*: After polynomial multiplication the accelerator applies polynomial addition and modulus switching. Polynomial addition is coefficient-wise addition of polynomials, taking one input from the INTT buffer and the other from a buffer filled by the RNG module. The output fills a small intermediate buffer that is the input to modulus switching, which removes the key-prime residue from the RNS encoding, resulting in  $k - 1$  polynomials. Modulus switching applies a series of modular multiplications and reductions, Modulus switching is the only operation that requires interaction across RNS residues, which precludes straightforward data parallelism across residues.

4) *Message Encoding*: After encrypting zero, CHOCO-TACO encodes, scales, and adds the input message to the encrypted zero. The encode/decode module includes a pair of small NTT and INTT blocks. The encoding hardware computes the modulus of each coefficient by the plaintext modulus  $t$ , and reorders coefficients into slots of the plaintext. The hardware must convert the encoded message to RNS, by scaling, representing it with  $k - 1$  residues only. A dedicated polynomial addition module adds the result to the  $k - 1$  intermediate residues of  $c_0$  and stores the result in the final output buffer.

5) *Memory*: Each module integrates and manages embedded SRAM scratchpad memory. All modules except NTT accept streaming inputs, and a module’s memories must accommodate its incoming (parallel) input stream at the rate of input arrivals and operation duration. NTT and INTT, however, algorithmically operate on an entire polynomial, requiring their buffers to be sized according to the HE scheme’s polynomial size. With HE parameters  $N = 8192$  and  $k = 3$ , each NTT/INTT buffer is 64kB. In contrast, other memories, sized via our design-space exploration in Section V are sub-1kB. As Section V explains, we model memories using Destiny, ported for single-reader, single-writer 64-byte data accesses.

## C. Encryption Operation Example

BFV encryption encrypts zero into a ciphertext and adds a scaled message to the encrypted-zero ciphertext. To start, the accelerator samples  $N$  bytes from the RNG according to a

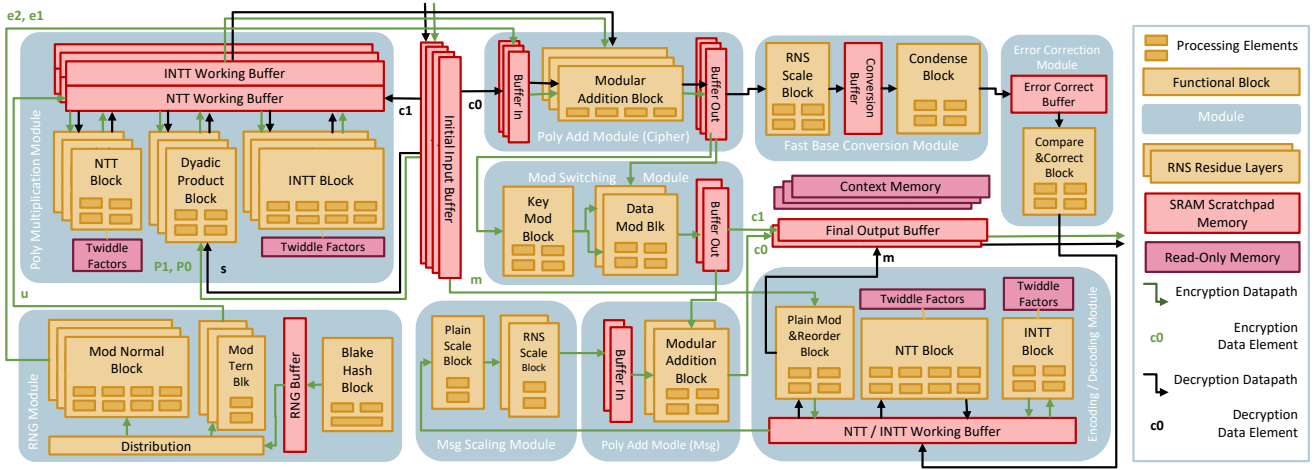


Fig. 7: Specialized architecture to support encryption & decryption for  $k = 3$

ternary distribution storing them in the NTT working buffer as  $u$ . The NTT block produces the NTT of  $u$  in place, and the value becomes the input to the dyadic product module. The dyadic product module's other input is the accelerator input buffer, which software initializes with the NTT-transformed residues of  $P1$ , a public key. Dyadic multiply produces the element-wise product of  $u$  and  $P1$  in the INTT block's buffer, which the INTT block processes.

In parallel with the dyadic product of  $u$  and  $P1$  the RNG unit produces  $e2$ , a sequence of 8-byte, normally distributed samples, storing them in a buffer in the cipher addition module. When the INTT completes, the PolyAdd module streams in its result, performing element-wise, addition with  $e2$  and storing the results in a buffer in the modulus switching module, as  $c1$ .

$c1$  is one component of the final ciphertext, which is output into the CPU's host memory

Meanwhile, the accelerator begins producing  $c0$  in the Poly Multiplication module. Computing  $c0$  reuses the NTT of  $u$ , performing element-wise multiplication with public key  $P0$ . The accelerator samples a sequence of normally-distributed 8-byte  $e1$  values (like  $e2$ ) adding them element-wise with the result of the INTT of the product of  $u$  and  $P0$ . The result is a partially-computed version of  $c0$ , the other component of the ciphertext.

The last step is the polynomial addition of the partially computed  $c0$  and the encoded input message, producing  $c0$ , which together with  $c1$  makes the final ciphertext.

#### D. Adding Parallelism

CHOCO-TACO exploits pipeline and data parallelism available in BFV encryption. Parallelism exists in independent RNS residues, independent coefficients and in pipelining throughout the accelerator.

Polynomial multiplication and addition manipulate the multiple residues of an RNS-encoded polynomial. Each of these residues is an independent share of the polynomial being manipulated and operations need to be applied identically to each residue. Up to the limits of area and power, a CHOCO-TACO

architecture can create parallel replicas of these operations' modules, including their input and output memories, enabling parallel processing of a polynomials RNS residues. RNS parallelism also eliminates the need to buffer the large vectors of random number for future execution. Instead,  $u$ ,  $e1$ , and  $e2$  are immediately consumed and distributed to all residues as they are generated. Figure 7 illustrates the parallelism of RNS residue operations graphically through layering.

Within each RNS layer, thousands of coefficients per polynomial afford data parallelism. A key design parameter for the CHOCO-TACO architecture is the degree to which each module exploits this source of data parallelism. Up to the limits of area and power, a CHOCO-TACO architecture can create parallel replicas of the blocks in a module, sizing memories to match, to enable higher throughput processing of coefficients. Section V systematically explores the design space of parallel accelerators.

#### E. Decryption Support

BFV decryption is operationally very similar to encryption. Equation 4 shows decryption mathematically.

$$Dec(s, [c0, c1]) = \left[ \left[ \frac{t}{q} [c0 + c1s]_q \right] \right]_t \quad (4)$$

Figure 7 shows the flow of control and data for decryption with black lines. Decryption requires a few additional hardware components, but reuses the existing polynomial multiplication and addition modules to process  $c1$ ,  $s$ , and  $c0$ . After addition, these intermediate results undergo fast base conversion and error correction, after which the message need only be decoded. Decoding uses the message encoding module, performing NTT, then moding by the plaintext modulus  $t$ . The result is the decrypted message, which the hardware conveys to the CPU's memory.

### V. ARCHITECTURAL DESIGN SPACE EXPLORATION

We explore the design space of the CHOCO-TACO hardware using a custom simulation infrastructure. The hardware

model captures the effects of parallelism and pipelining and estimates time, power, area, and energy. We implemented individual hardware components in RTL and synthesized them with Cadence Genus, in a generic 45nm technology node. We modeled three-stage, pipelined multiplication and division units. To model memory, we used Destiny [38], modeling SRAMs using its aggressive wire technology, optimized for read energy with 8-word, 64-byte, memory accesses. The access latency of our energy-optimized memories limits clock frequency, and we clocked the design at 100 MHz.

### A. Performance Tradeoffs

We quantified the tradeoff of area, time, and power, with a systematic exploration of the CHOCO-TACO hardware design space. Using our simulator, we swept across 31,340 different architectural configurations. For each block in each module, the study varied the number of processing elements from one to 16 in powers of two, varying memory capacity commensurately, between 128 and 1024 bytes per RNS-parallel layer, except for NTT/INTT units, which require a fixed memory size. For each configuration, the study assessed power (leakage & average dynamic), area, energy and compute time for a single encryption operation. Results from the design exploration are presented in Figure 8.

Overall, the design space shows significant variation in power and area, with a marked Pareto frontier along which power, time, and area balance. We selected an operating point for CHOCO-TACO by limiting power to 200 mW, and choosing the smallest design that had a run time within 1% of the best run time (and energy). The chosen configuration has 19.3 mm<sup>2</sup> area and consumes .1228 mJ to perform a single encryption in .66 ms. Figure 7 depicts this configuration graphically.

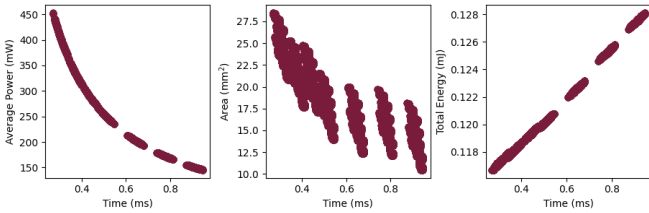


Fig. 8: Design space for encryption hardware with respect to power, area, and energy. Parallelism tradeoffs are available in multiple dimensions at each stage of the encryption pipeline.

### B. CHOCO-TACO Makes Encryption Fast and Low-Energy

We evaluated the benefit in time and energy of CHOCO-TACO for encryption compared to a software encryption baseline, showing that across a range of HE parameter settings, hardware support provides substantial improvements. Figure 9 shows data comparing software encryption to encryption with hardware acceleration. We evaluated the default HE parameter settings of SEAL, as well as CHOCO’s parameter setting of (8192, 3), as presented in Table III. The baseline is an average of 100 encryption operations running in software on our IMX6

hardware. Results are shown in Figure 9. We omit baseline data for the (32768,16) parameter setting because the IMX6 board does not have enough memory to encrypt data for these parameters. Notably, this configuration with its prohibitive memory requirements is not uncommon in existing encrypted inference solutions [14], [15]

For the CHOCO (8192, 3) configuration, CHOCO-TACO provides an improvement over the software baseline of 417 $\times$  in time and 603 $\times$  in energy. The data also show a performance scaling trend, in that with hardware support, encryption time scales up directly with  $N$ , while software scales up with both  $N$  and  $k$ . The scalability benefits comes from parallelism in the accelerator architecture: replicated modules process independent RNS residues in parallel. Decryption sees less benefit from hardware acceleration than encryption, with only a 125 $\times$  speedup over software for the (8192,3) CHOCO parameter selection. This decrease in speedup is contributed to limited parallelism because decryption operates on only a single polynomial at this parameter selection.

Overall, CHOCO-TACO provides up to 1094 $\times$  and 648 $\times$  savings in time and energy, respectively, and providing consistent gains across HE parameter settings.

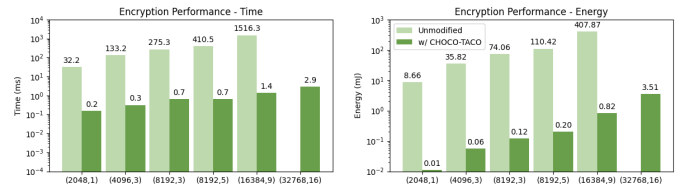


Fig. 9: Logarithmic comparison of time & energy of the CHOCO-TACO architecture presented in Figure 7 for varying encryption parameters versus a 528MHz device w/o dedicated hardware support.

## VI. EVALUATION

We evaluate CHOCO to show the importance of algorithm optimization and architectural acceleration to the practicality of resource-constrained devices participating in client-aided privacy preserving computation. In accordance with prior work, we evaluate CHOCO using several large-scale machine learning models. We show reduction of communication overhead by up to three orders of magnitude over existing state of the art privacy-preserving DNN inference solutions. This is a direct result of the smaller parameter selections enabled by CHOCO optimizations, including rotational redundancy. Additionally, we show that the comprehensive hardware acceleration provided by CHOCO-TACO improves the runtime of active client computation by an additional 54.3 $\times$  than dedicated NTT/INTT and dyadic product acceleration alone. Ultimately, we demonstrate that a complete CHOCO implementation using Bluetooth communication is comparable to local computation with TensorFlow Lite and, for large networks, reduces inference energy by up to 37%.

### A. Applications & Methodology

1) *Neural Network Selection:* We evaluate CHOCO for DNN inference, implementing client-aided, encrypted versions

of the four image classification DNNs in Table V. The Lenet variants operate on MNIST data [39], and the other, larger networks classify CIFAR-10 images [40]. We trained the DNNs on unencrypted data using standard quantization-aware training in Tensorflow 2.2.0 [41]. Evaluations are performed by running single-image inference through each network.

TABLE V: Neural Networks used for system evaluation

Network	# Layers				MACs ( $\times 10^6$ )	% Acc.			Mod. Sz. (MB)		Comm. (MB)
	Cnv	FC	Act	Pl		Float	8b	4b	Float	4b	
LeNetSm [42]	2	1	2	2	0.24	99.0	94.9	93.8	0.02	0.01	0.66
LeNetLg [43]	2	2	3	2	12.27	98.7	97.2	96.4	8.22	2.07	2.6
SqzNet [44]	10	0	10	3	32.60	76.5	74.0	15.0	0.57	0.16	13.8
VGG16 [45]	13	2	14	5	313.26	70.0	66.0	21.0	56.40	14.13	22.2

2) *Client Modeling*: We perform baseline client evaluations for software running on an NXP IMX6 evaluation kit with an ARM Cortex-A7 CPU at 528MHz, 32/128 kB of L1/L2 cache, and 4 GB DDR3L SDRAM. We estimate power and energy using an average power characterization (running Dhrystone) of 269.5 mW from the manufacturer’s Application Note AN5345 [46]. We follow the methodology from Section II to estimate HEAX acceleration and use the hardware configuration from Section V to model CHOCO-TACO acceleration.

### B. CHOCO Optimizations Reduce Communication

The algorithmic optimizations presented in Section III-B, including rotational redundancy, minimize noise growth to enable smaller parameter selections and correspondingly smaller ciphertexts. As discussed in Section II-A, all of the networks included in Table V can be evaluated in CHOCO using ciphertexts with no more than 8192 elements ( $N = 8192$ ). This is in contrast to existing HE solutions [14]–[16], [18], [20], [21] which commonly use ciphertexts of 16 or even 32 thousand elements. By eliminating unnecessary prime residues, CHOCO further reduces ciphertext size by another 50% over SEAL’s default parameters at  $N = 8192$ .

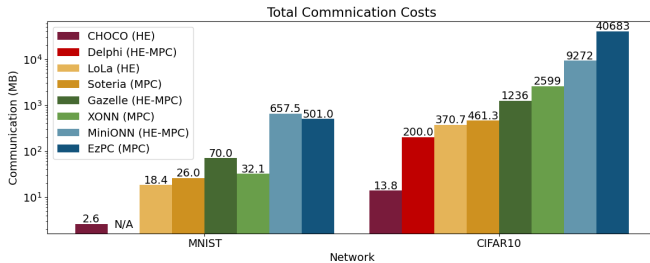


Fig. 10: Comparison of total communication requirements to perform single image inference via the Lenet-5-Large (MNIST) and SqueezeNet (CIFAR-10) implementations in CHOCO and comparable networks in several state of the art privacy-preserving DNN protocols.

This reduction in ciphertext size directly translates to improvements in server runtime, client responsibility (Figure 11), and communication overhead. Figure 10 demonstrates the communication improvement over several state of the art

privacy-preserving DNN protocols. Comparisons are evaluated between the CHOCO implementations of Lenet-5-Large and SqueezeNet and comparable networks performing MNIST and CIFAR-10 single-image inference, respectively. They include communication for both offline preprocessing and online computation. Although the networks evaluated in this work are substantially larger (more model parameters) in all cases, CHOCO outperforms existing protocols by up to three orders of magnitude. Because of the smaller parameter selections and more efficient ciphertext packing, benefits are witnessed even compared to LoLa [14], a *non-client-aided* encrypted inference protocol. For the most closely comparable protocol, namely Gazelle [18], CHOCO still provides a nearly 90 $\times$  improvement in communication overhead. This reduction dramatically reduces end-to-end latency, especially for IoT devices often communicating over lower bandwidth channels such as Bluetooth.

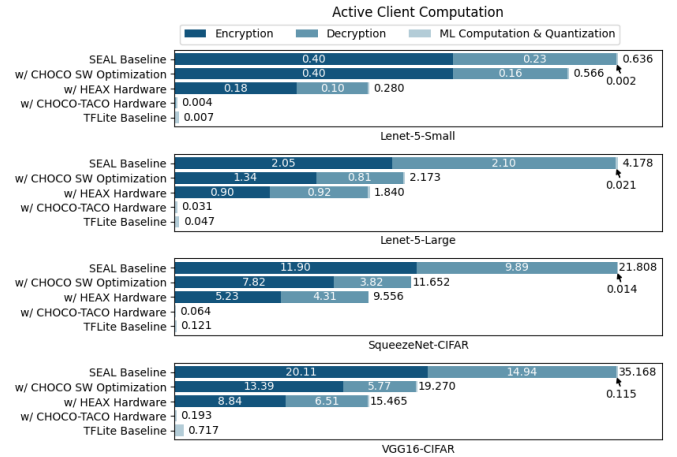


Fig. 11: Extension of client execution times shown in Figure 3 including CHOCO execution time breakdown.

### C. CHOCO-TACO Accelerates Client Computation

We evaluate our hardware setup running single-image inference. We compare it to both the software optimized baseline and the baseline equipped with HEAX’s NTT unit and Dyadic Multiply unit only. The software optimized baseline includes the algorithmic optimizations of CHOCO, namely rotational redundancy, and already demonstrates an average 1.7 $\times$  improvement over the SEAL baseline software with standard permutations and default parameter selections. A baseline that runs local inference on the ARM Cortex-A7 CPU using TensorFlow Lite (TFLite) software is also included as a lower-bound. We compute time and energy savings for active client computation by counting the number of encryption and decryption operations necessary to run inference for each network, and multiplying by the cost of each operation. We assume that the time for client computation and quantization, including ReLu and Pooling, stays the same for CHOCO as in the baseline. Figure 11 reports the resulting execution times, breaking down the total time into its constituent components.

The data show an average speedup of  $121\times$  over the optimized software baseline for computations on the client, which is consistent with the  $417\times$  and  $125\times$  speedups observed for encryption and decryption, respectively.

The data clearly show that encryption and decryption are the bottleneck on the client. NTT and Dyadic multiply only account for roughly 50% of these operations. Thus, dedicated hardware units for these sub-operations alone, including but not limited to those provided by HEAX [31], is not enough. The cryptographic operations for a client-aided protocol are still  $25\times$  slower on average than computing the entire network locally with TF Lite.

Comprehensive hardware acceleration for encryption and decryption is imperative. CHOCO-TACO recognizes this and uses an optimal allocation of compute resources, minimal buffering, tightly integrated memories, and multiple levels of parallelism to address the remaining 50% of computation. With the acceleration provided by CHOCO-TACO, the time of active client computation on client-aided encrypted DNN inference becomes  $2.2\times$  faster on average than local inference.

#### D. Full Implementation Comparable to Local Compute

To understand the end-to-end benefits, we study a reference implementation of CHOCO that communicates between the client and the offload using 10mW Bluetooth communication at 22 Mbps [47]. Timing and energy results follow analytically from the data communication requirements, included in Table V, of each network. End-to-end time and energy results are compared against the TFLite baseline in Figure 12. The data show that in a full implementation communication time begins to dominate. For low-power, low-data-rate protocols such as Bluetooth, communication presents a  $24\times$  average time overhead compared to local compute. However, in small devices battery preservation often outweighs the need for fast compute. In energy consumption CHOCO is competitive with the TFLite baseline. For VGG, the largest and most complex of the DNNs evaluated, CHOCO earns up to a 37% end-to-end decrease in energy consumption.

The data carry several main take-away points. The first take-away is that hardware acceleration, like CHOCO-TACO is essential to make feasible the CHOCO model for client-aided encrypted computing. Without our hardware acceleration — even with the partial acceleration from HEAX [31] — encryption and decryption are the computing and energy bottleneck. Our hardware support accelerates the entire encryption and decryption computation, driving its cost down, eliminating it as the bottleneck, and making CHOCO feasible. Second, intentional client-aware optimizations are essential to bring privacy-preserving computation to resource-constrained IoT clients. Although communication remains a key bottleneck in time and energy, the algorithmic optimizations of CHOCO reduce this cost by up to three orders of magnitude. For the first time, this dramatic reduction makes client time and energy requirements competitive with local inference, even displaying the possibility of end-to-end gains. Third, the benefit of CHOCO-TACO depends on the structure of the computation:

VGG sees substantial performance and energy improvements, while SqueezeNet sees a break-even or loss. We characterize this workload-dependent benefit in the next section.

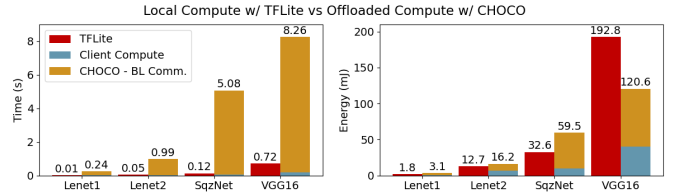


Fig. 12: Client execution time & energy for single image inference via local compute using TFLite software and offloaded compute using a full hardware-software reference implementation of CHOCO-TACO using Bluetooth communication.

#### E. Network Design

Different workloads see different benefit from CHOCO computation, which owes to differences in the rates of computation and communication required by these different workloads. CHOCO using Bluetooth communication for VGG sees a 37% energy savings, while SqueezeNet sees a 82.5% energy overhead. We performed a microbenchmarking study to evaluate this influence of workload structure. We constructed workloads with a variety of different convolutional DNN layers of different dimensions. The structure of the convolutional layers varies the number of multiply-accumulate (MAC) operations performed by each layer, as well as the amount of communication required to send and receive the ciphertexts that contain each layer’s inputs. Figure 13 shows the results of this study, plotting these microbenchmark convolution points, as well as each of the layers from VGG and from SqueezeNet. For the microbenchmark points, we varied image size from 2 to 32 by powers of two, varied image channel values from 32 to 512 by powers of 2. Following the implementations of SqueezeNet and VGG16, we used filter sizes of 3 or 1. The data show that workloads like VGG (which are likely to see its same energy benefits) are ones that maximize the number of MACs per MB of communication. Workloads like SqueezeNet (which are likely to see its break-even or costs) are ones that have fewer MACs per MB of communication.

These data provide two main benefits in interpreting CHOCO. First, the data show that a quick analytical comparison of computation (MACs) versus communication (MBs) per layer helps an application designer decide if their DNN application will see an energy benefit in the CHOCO client-aided model. Second, the data point to an opportunity for future work, optimizing DNN structure to maximize compute per communication for the CHOCO model.

#### F. CHOCO with Model Privacy

CHOCO targets a use case with relaxed model security requirements, and optimizes for minimal client-side computation and communication. However, when model security is a strict necessity, many optimizations presented would also benefit a client participating in a hybrid HE-MPC protocol.

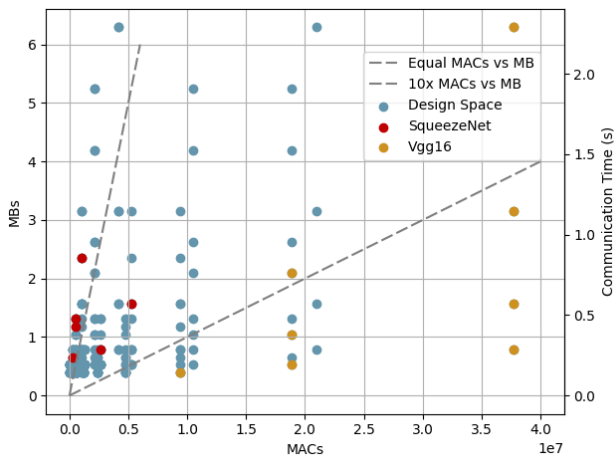


Fig. 13: Communication vs Computation for Convolution Layers of a DNN with different parameters

Namely, rotational redundancy can be applied to any HE algorithms using windowed rotations to reduce noise growth and enable smaller parameter selections, thus providing similar improvements in computation and communication to other protocols. Additionally, in any client-aided model encryption and decryption will repeatedly fall along the critical path. Therefore, hardware acceleration such as that presented in CHOCO-TACO will continue to be beneficial in reducing the time and energy required for these critical operations.

## VII. RELATED WORKS

### A. Privacy Preserving DNN Inference

ML offloading requires data privacy. Recent work optimized server-centric metrics, including usability [15], [16], training [48], throughput (via batching) [16], [17], [30], latency (via packing) [14], [15], [18], [49], network complexity [17], [18], [20], performance [31]–[33], and model privacy [11]–[13], [18]–[21]. Unlike prior work that focused on the server, to the best of our knowledge, CHOCO is the first work optimizing for resource-constrained client devices in client-aided HE.

### B. HE Hardware Support

Some prior work used hardware to accelerate kernels for lattice-based cryptography schemes [50]–[53], including current state-of-art schemes [23]–[26]. Some directly accelerate HE [31], [32], [34], [54], focusing primarily on hardware NTT. As we show in Figure 3, NTT acceleration helps but is insufficient. Our work is the first to *comprehensively* optimize HE cryptographic primitives, which is crucial in client-aided HE. Furthermore, unlike prior work targeting large, high-power GPUs [55]–[57] and FPGAs [31]–[34], CHOCO opts for an ASIC implementation, directly addressing the need for low-power, energy-efficient operation at the client device.

### C. Hardware Security

Recent architectures offer privacy-preserving offloaded computation. Some techniques ensure data privacy, such as

Trusted Execution Environments (TEEs) [8]–[10] and memory access control and obfuscation [58]–[61]. While these prior techniques are vulnerable to side channel attacks, HE is not and data remain private while offloaded; HE is favorable thanks to its strong, proven privacy guarantee. Moreover, client-aided HE allows interactions between the client and server that are not allowed by TEEs [8].

### D. Low-Power ML Acceleration

Client DNN inference performance is improving through software [41], [62] and hardware optimization [63], [64]. One alternative to HE for private inference is to simply outfitting IoT devices with local ML acceleration and computing locally. However, as we argue in Section II, local compute imposes tight resource limits and requires maintaining (i.e., updating) models on a potentially very large number of client devices, rather than an offload server’s centralized model. In contrast, CHOCO targets encrypted offload of ML (and other) computations, imposing few restrictions on centrally managed models. Furthermore, CHOCO’s support straightforwardly generalizes beyond ML: outfitting a device with a HE cryptographic accelerator, rather specialized DNN hardware, enables participating in *any* client-aided, encrypted computation, not only ML. Encrypted applications research is an active, emerging area [48], [65]–[68]; CHOCO-TACO benefits a broad set of existing and future encrypted applications.

## VIII. CONCLUSION

In this work we present CHOCO, Client-aided HE for Opaque Compute Offloading, a client-optimized system for privacy-preserving collaborative computing that enables participation from resource-constrained IoT client devices. We show that selecting efficient encryption parameters is critical to the performance of such a system and present rotational redundancy as an encrypted algorithm optimization to allow for more efficient selections. Because of its ability to use smaller ciphertexts, CHOCO reduces communication overheads by up to three orders of magnitude over existing privacy-preserving DNN inference protocols. Motivated by the remaining client computation bottleneck, we introduce CHOCO-TACO, hardware support to accelerate HE encryption and decryption along the critical path. By exploiting parallelism and supporting local data storage, CHOCO-TACO boasts a  $417\times$  speedup and a  $603\times$  energy savings for a single encryption operation. When integrated back into the full CHOCO system this translates to a  $121\times$  speedup on average for the client-side compute of DNN inference. For a reference implementation using Bluetooth communication, the combined hardware and software benefits from CHOCO-TACO make collaborative encrypted computing competitive against local compute with TFLite. A previously insurmountable task, this work, through its intentional client-aware optimizations, demonstrates that participation from resource-constrained IoT clients in collaborative encrypted computing is both feasible and even favorable.

## REFERENCES

- [1] H.-J. Chae, D. Yeager, J. Smith, and K. Fu, "Wirelessly powered sensor networks and computational rfid," 01 2013.
- [2] A. Colin, E. Ruppel, and B. Lucia, "A reconfigurable energy storage architecture for energy-harvesting devices," *SIGPLAN Not.*, vol. 53, no. 2, p. 767–781, Mar. 2018. [Online]. Available: <https://doi.org/10.1145/3296957.3173210>
- [3] J. D. Garside, S. B. Furber, S. Temple, and J. V. Woods, "The amulet chips: Architectural development for asynchronous microprocessors," in *2009 16th IEEE International Conference on Electronics, Circuits and Systems - (ICECS 2009)*, 2009, pp. 343–346.
- [4] S. Liu, K. Pattabiraman, T. Moscibroda, and B. G. Zorn, "Flicker: Saving dram refresh-power through critical data partitioning," *SIGARCH Comput. Archit. News*, vol. 39, no. 1, p. 213–224, Mar. 2011. [Online]. Available: <https://doi.org/10.1145/1961295.1950391>
- [5] P. Sparks, "The route to a trillion devices: The outlook for iot investment to 2035," arm, Tech. Rep., June 2017, <https://community.arm.com/iot/b/internet-of-things/posts/white-paper-the-route-to-a-trillion-devices>.
- [6] N. Jackson and P. Dutta, "Permacam: A wireless camera sensor platform for multi-year indoor computer vision applications," [https://conix.io/wp-content/uploads/pubs/3113/jackson\\_permacam\\_conix\\_2020.pptx.pdf](https://conix.io/wp-content/uploads/pubs/3113/jackson_permacam_conix_2020.pptx.pdf), Oct 2020.
- [7] M. Nardello, H. Desai, D. Brunelli, and B. Lucia, "Camaroptera: A batteryless long-range remote visual sensing system," in *Proceedings of the 7th International Workshop on Energy Harvesting & Energy-Neutral Sensing Systems*, ser. ENSys'19. New York, NY, USA: Association for Computing Machinery, 2019, p. 8–14. [Online]. Available: <https://doi.org/10.1145/3362053.3363491>
- [8] I. Corporation, *Intel 64 and IA-32 Architectures Software Developer's Manual*, Nov 2020.
- [9] J. Park, N. Kang, T. Kim, Y. Kwon, and J. Huh, "Nested enclave: Supporting fine-grained hierarchical isolation with sgx," in *Proceedings of the ACM/IEEE 47th Annual International Symposium on Computer Architecture*, ser. ISCA '20. IEEE Press, 2020, p. 776–789. [Online]. Available: <https://doi.org/10.1109/ISCA45697.2020.00069>
- [10] P. Subramanyan, R. Sinha, I. Lebedev, S. Devadas, and S. A. Seshia, "A formal foundation for secure remote execution of enclaves," in *Proceedings of the 2017 ACM SIGSAC Conference on Computer and Communications Security*, ser. CCS '17. New York, NY, USA: Association for Computing Machinery, 2017, p. 2435–2450. [Online]. Available: <https://doi.org/10.1145/3133956.3134098>
- [11] A. Aggarwal, T. E. Carlson, R. Shokri, and S. Tople, "Soteria: In search of efficient neural networks for private inference," 2020.
- [12] M. S. Riazi, M. Samragh, H. Chen, K. Laine, K. Lauter, and F. Koushanfar, "XONN: Xnor-based oblivious deep neural network inference," in *28th USENIX Security Symposium (USENIX Security 19)*. Santa Clara, CA: USENIX Association, Aug. 2019, pp. 1501–1518. [Online]. Available: <https://www.usenix.org/conference/usenixsecurity19/presentation/riazi>
- [13] N. Chandran, D. Gupta, A. Rastogi, R. Sharma, and S. Tripathi, "Ezpc: Programmable, efficient, and scalable secure two-party computation for machine learning," Cryptology ePrint Archive, Report 2017/1109, 2017, <https://eprint.iacr.org/2017/1109>.
- [14] A. Brutzkus, O. Elisha, and R. Gilad-Bachrach, "Low latency privacy preserving inference," in *International Conference on Machine Learning*, 2019.
- [15] R. Dathathri, O. Saarikivi, H. Chen, K. Laine, K. Lauter, S. Maleki, and T. Musuvathi, M. Mytkowicz, "Chet: An optimizing compiler for fully-homomorphic neural-network inferencing," in *40th ACM SIGPLAN Conference on Programming Language Design and Implementation (PLDI)*. ACM, June 2019.
- [16] N. Dowlin, R. Gilad-Bachrach, K. Laine, K. Lauter, M. Naehrig, and J. Wernsing, "Cryptonets: applying neural networks to encrypted data with high throughput and accuracy," in *33rd International Conference on Machine Learning (ICML)*. ACM, June 2016.
- [17] F. Boemer, A. Costache, R. Cammarota, and C. Wierzynski, "nGraph-HE2: A high-throughput framework for neural network inference on encrypted data," Aug 2019, arXiv:1908.04172v2.
- [18] C. Juvekar, V. Vaikuntanathan, and A. Chandrakasan, "Gazelle: A low latency framework for secure neural network inference," in *Proceedings of the 27th USENIX Conference on Security Symposium*, ser. SEC'18. USA: USENIX Association, 2018, p. 1651–1668.
- [19] P. Mishra, R. Lehmkuhl, A. Srinivasan, W. Zheng, and R. A. Popa, "Delphi: A cryptographic inference service for neural networks," in *29th USENIX Security Symposium (USENIX Security 20)*. USENIX Association, Aug. 2020, pp. 2505–2522. [Online]. Available: <https://www.usenix.org/conference/usenixsecurity20/presentation/mishra>
- [20] J. Liu, M. Juuti, Y. Lu, and N. Asokan, "Oblivious neural network predictions via minion transformations," in *Proceedings of the 2017 ACM SIGSAC Conference on Computer and Communications Security*, ser. CCS '17. New York, NY, USA: Association for Computing Machinery, 2017, p. 619–631. [Online]. Available: <https://doi.org/10.1145/3133956.3134056>
- [21] B. Reagen, W. Choi, Y. Ko, V. Lee, G.-Y. Wei, H.-H. S. Lee, and D. Brooks, "Cheetah: Optimizing and accelerating homomorphic encryption for private inference," 2020.
- [22] J. Fan and F. Vercauteren, "Somewhat practical fully homomorphic encryption," Cryptology ePrint Archive, Report 2012/144, 2012, <https://eprint.iacr.org/2012/144>.
- [23] J. H. Cheon, A. Kim, M. Kim, and Y. Song, "Homomorphic encryption for arithmetic of approximate numbers," Cryptology ePrint Archive, Report 2016/421, 2016, <https://eprint.iacr.org/2016/421>.
- [24] C. Gentry, "Fully homomorphic encryption using ideal lattices," in *Proceedings of the 41st Annual ACM Symposium on Theory of Computing*, ser. STOC 41. New York, NY, USA: Association for Computing Machinery, 2009, pp. 169–178.
- [25] Z. Brakerski, "Fully homomorphic encryption without modulus switching from classical gapsvp," in *Proceedings of the 32nd Annual Cryptology Conference on Advances in Cryptology — CRYPTO 2012 - Volume 7417*. Berlin, Heidelberg: Springer-Verlag, 2012, p. 868–886. [Online]. Available: [https://doi.org/10.1007/978-3-642-32009-5\\_50](https://doi.org/10.1007/978-3-642-32009-5_50)
- [26] J. Fan and F. Vercauteren, "Somewhat practical fully homomorphic encryption," Cryptology ePrint Archive, Report 2012/144, 2012, <https://eprint.iacr.org/2012/144>.
- [27] "Microsoft SEAL (release 3.4)," <https://github.com/Microsoft/SEAL>, Oct 2019, microsoft Research, Redmond, WA.
- [28] K. Laine, *Simple Encrypted Arithmetic Library 2.3.1*, Microsoft Research, 2017.
- [29] J. C. Bajard, N. Meloni, and T. Plantard, "Efficient rns bases for cryptography," 07 2005.
- [30] E. Hesamifard, H. Takabi, and M. Ghasemi, "Deep neural networks classification over encrypted data," in *Proceedings of the Ninth ACM Conference on Data and Application Security and Privacy*, ser. CODASPY '19. New York, NY, USA: Association for Computing Machinery, 2019, p. 97–108. [Online]. Available: <https://doi.org/10.1145/3292006.3300044>
- [31] M. S. Riazi, K. Laine, B. Pelton, and W. Dai, "Heax: An architecture for computing on encrypted data," in *Proceedings of the Twenty-Fifth International Conference on Architectural Support for Programming Languages and Operating Systems*, ser. ASPLOS '20. New York, NY, USA: Association for Computing Machinery, 2020, p. 1295–1309. [Online]. Available: <https://doi.org/10.1145/3373376.3378523>
- [32] F. Turan, S. S. Roy, and I. Verbauwhede, "Heaws: An accelerator for homomorphic encryption on the amazon aws fpga," *IEEE Transactions on Computers*, vol. 69, no. 8, pp. 1185–1196, 2020.
- [33] S. S. Roy, F. Turan, K. Jarvinen, F. Vercauteren, and I. Verbauwhede, "Fpga-based high-performance parallel architecture for homomorphic computing on encrypted data," Cryptology ePrint Archive, Report 2019/160, 2019, <https://eprint.iacr.org/2019/160>.
- [34] A. Mert, E. Ozturk, and E. Savas, "Design and implementation of encryption/decryption architectures for bfv homomorphic encryption scheme," *IEEE Transactions on Very Large Scale Integration (VLSI) Systems*, vol. 28, no. 02, pp. 353–362, feb 2020.
- [35] N. Zmora, G. Jacob, L. Zlotnik, B. Elharar, and G. Novik, "Neural network distiller: A python package for dnn compression research," October 2019, <https://arxiv.org/abs/1910.12232>.
- [36] S. Halevi and V. Shoup, "Algorithms in helib," Cryptology ePrint Archive, Report 2014/106, 2014, <https://eprint.iacr.org/2014/106>.
- [37] J. O'Connor, S. Neves, J.-P. Aumasson, and Z. Wilcox-O'Hearn, "Blake3," <https://github.com/BLAKE3-team/BLAKE3>, 2019.
- [38] M. Poremba, S. Mittal, D. Li, J. S. Vetter, and Y. Xie, "Destiny: A tool for modeling emerging 3d nvm and edram caches," in *2015 Design, Automation Test in Europe Conference Exhibition (DATE)*, 2015, pp. 1543–1546.

- [39] Y. LeCun, C. Cortes, and C. Burges, "Mnist handwritten digit database," *ATT Labs [Online]*. Available: <http://yann.lecun.com/exdb/mnist>, vol. 2, 2010.
- [40] A. Krizhevsky, "Learning multiple layers of features from tiny images," University of Toronto, Tech. Rep., 2009.
- [41] M. Abadi *et al.*, "TensorFlow: Large-scale machine learning on heterogeneous systems (release 2.2)," 2015, <https://www.tensorflow.org/>.
- [42] E. Freiman, "Digit recognizer for mlpack," 2018, <https://github.com/mlpack/models/tree/master/Kaggle>.
- [43] Tensorflow, "Lenet-5-like convolutional mnist model example," 2016, <https://github.com/tensorflow/models/blob/v1.9.0/tutorials/image/mnist/convolutional.py>.
- [44] D. Corvoysier, "Squeezenet for cifar-10," 2017, <https://github.com/kaizouman/tensorsandbox/tree/master/cifar10/models/squeeze>.
- [45] S. Liu and W. Deng, "Very deep convolutional neural network based image classification using small training sample size," pp. 730–734, Nov 2015.
- [46] N. Semiconductors, "Imx6ull power consumption application note," arm, Tech. Rep. AN5345-2, 10 2016, <https://www.nxp.com/docs/en/application-note/AN5345.pdf>.
- [47] Y. Mao, C. You, J. Zhang, K. Huang, and K. B. Letaief, "A survey on mobile edge computing: The communication perspective," *IEEE Communications Surveys Tutorials*, vol. 19, no. 4, pp. 2322–2358, 2017.
- [48] P. Mohassel and Y. Zhang, "Secureml: A system for scalable privacy-preserving machine learning," in *IEEE Symposium on Security and Privacy (SP)*. IEEE, May 2017, pp. 19–38.
- [49] M. S. Riazzi, C. Weinert, O. Tkachenko, E. M. Songhori, T. Schneider, and F. Koushanfar, "Chameleon: A hybrid secure computation framework for machine learning applications," *CoRR*, vol. abs/1801.03239, 2018. [Online]. Available: <http://arxiv.org/abs/1801.03239>
- [50] S. Roy, F. Vercauteren, N. Mentens, D. Chen, and I. Verbauwhede, "Compact ring-lwe cryptoprocessor," in *Proceedings of the 16th International Workshop on Cryptographic Hardware Embedded Systems (CHES)*. Springer, Sep 2014, pp. 371–391.
- [51] R. de Clercq, S. Roy, F. Vercauteren, and I. Verbauwhede, "Efficient software implementation of ring-lwe encryption," in *DATE*, Mar 2015, pp. 339–344.
- [52] C. Renteria-Mejia and J. Velasco-Medina, "High-throughput ring-lwe cryptoprocessors," *IEEE Transactions on Very Large Scale Integration (VLSI) Systems*, vol. 25, no. 08, pp. 2332–2345, aug 2017.
- [53] P. Longa and M. Naehrig, "speeding up the number theoretic transform for faster ideal lattice-based cryptography," in *Cryptology and Network Security*. Springer, Nov 2016, pp. 124–139.
- [54] S. Kim, K. Lee, W. Cho, Y. Nam, J. H. Cheon, and R. A. Rutenbar, "Hardware architecture of a number theoretic transform for a bootstrappable rns-based homomorphic encryption scheme," in *2020 IEEE 28th Annual International Symposium on Field-Programmable Custom Computing Machines (FCCM)*, 2020, pp. 56–64.
- [55] W. Dai and B. Sunar, "cuhe: A homomorphic encryption accelerator library," in *Cryptography and Information Security in the Balkans*. Springer International Publishing, 2015, pp. 169–186.
- [56] A. A. Badawi, V. Veeravalli, C. Mun, and K. Aung, "High-performance fv somewhat homomorphic encryption on gpus: An implementation using cuda," in *CHES*, vol. 2018, no.2, 2018, pp. 70–95.
- [57] A. Qaisar Ahmad Al Badawi, Y. Polyakov, K. M. M. Aung, B. Veeravalli, and K. Rohloff, "Implementation and performance evaluation of rns variants of the bfv homomorphic encryption scheme," *IEEE Transactions on Emerging Topics in Computing*, pp. 1–1, 2019.
- [58] L. Ren, X. Yu, C. W. Fletcher, M. van Dijk, and S. Devadas, "Design space exploration and optimization of path oblivious ram in secure processors," in *Proceedings of the 40th Annual International Symposium on Computer Architecture*, ser. ISCA '13. New York, NY, USA: Association for Computing Machinery, 2013, p. 571–582. [Online]. Available: <https://doi.org/10.1145/2485922.2485971>
- [59] H. Sasaki, M. A. Arroyo, M. T. I. Ziad, K. Bhat, K. Sinha, and S. Sethumadhavan, "Practical byte-granular memory blacklisting using califorms," in *Proceedings of the 52nd Annual IEEE/ACM International Symposium on Microarchitecture*, ser. MICRO '52. New York, NY, USA: Association for Computing Machinery, 2019, p. 558–571. [Online]. Available: <https://doi.org/10.1145/3352460.3358299>
- [60] A. Shafiq, R. Balasubramanian, M. Tiwari, and F. Li, "Secure dimm: Moving oram primitives closer to memory," in *2018 IEEE International Symposium on High Performance Computer Architecture (HPCA)*, 2018, pp. 428–440.
- [61] C. Hunger, L. Vilanova, C. Papamanthou, Y. Etsion, and M. Tiwari, "Dats - data containers for web applications," in *Proceedings of the Twenty-Third International Conference on Architectural Support for Programming Languages and Operating Systems*, ser. ASPLOS '18. New York, NY, USA: Association for Computing Machinery, 2018, p. 722–736. [Online]. Available: <https://doi.org/10.1145/3173162.3173213>
- [62] A. Paszke, S. Gross, F. Massa, A. Lerer, J. Bradbury, G. Chanan, T. Killeen, Z. Lin, N. Gimelshein, L. Antiga, A. Desmaison, A. Kopf, E. Yang, Z. DeVito, M. Raison, A. Tejani, S. Chilamkurthy, B. Steiner, L. Fang, J. Bai, and S. Chintala, "Pytorch: An imperative style, high-performance deep learning library," in *Advances in Neural Information Processing Systems 32*, H. Wallach, H. Larochelle, A. Beygelzimer, F. d'Alché-Buc, E. Fox, and R. Garnett, Eds. Curran Associates, Inc., 2019, pp. 8024–8035. [Online]. Available: <http://papers.neurips.cc/paper/9015-pytorch-an-imperative-style-high-performance-deep-learning-library.pdf>
- [63] Y. Chen, J. Emer, and V. Sze, "Eyeriss: A spatial architecture for energy-efficient dataflow for convolutional neural networks," in *2016 ACM/IEEE 43rd Annual International Symposium on Computer Architecture (ISCA)*, 2016, pp. 367–379.
- [64] S. Han, X. Liu, H. Mao, J. Pu, A. Pedram, M. A. Horowitz, and W. J. Dally, "Eie: Efficient inference engine on compressed deep neural network," in *2016 ACM/IEEE 43rd Annual International Symposium on Computer Architecture (ISCA)*, 2016.
- [65] J. Wang, A. Arriaga, Q. Tang, and P. Y. Ryan, "Facilitating privacy-preserving recommendation-as-a-service with machine learning," in *Proceedings of the 2018 ACM SIGSAC Conference on Computer and Communications Security*, ser. CCS '18. New York, NY, USA: Association for Computing Machinery, 2018, p. 2306–2308. [Online]. Available: <https://doi.org/10.1145/3243734.3278504>
- [66] G. S. Çetin, Y. Doröz, B. Sunar, and E. Savaş, "Low depth circuits for efficient homomorphic sorting," *Cryptology ePrint Archive, Report 2015/274*, 2015, <https://eprint.iacr.org/2015/274>.
- [67] F. Baldimtsi and O. Ohrimenko, "Sorting and searching behind the curtain: Private outsourced sort and frequency-based ranking of search results over encrypted data," *Cryptology ePrint Archive, Report 2014/1017*, 2014, <https://eprint.iacr.org/2014/1017>.
- [68] y. GUO, X. Yuan, X. Wang, C. Wang, B. Li, and X. Jia, "Enabling encrypted rich queries in distributed key-value stores," *IEEE Transactions on Parallel and Distributed Systems*, vol. 30, no. 6, pp. 1283–1297, 2019.